Structural Determinants of the Packing and Electrostatic Behavior of Unsaturated Phosphoglycerides

Howard L. Brockman,* Maureen M. Momsen,* Weiling C. King,† and John A. Glomset†
*Hormel Institute, University of Minnesota, Austin, Minnesota 55912; and †Howard Hughes Medical Institute, Departments of Medicine and Biochemistry and Regional Primate Research Center, University of Washington, Seattle, Washington 98195

ABSTRACT Docosahexaenoic acid-containing phosphoglycerides accumulate preferentially in membranes of the retina, brain, and spermatozoa, but the functional significance of this largely remains to be determined. Previously we compared the physical properties of homogeneous monolayers of these and other phosphoglyceride species to obtain insights into their physiological roles. Particularly noteworthy were the unusually low dipole moments of species having *sn*-2-docosahexaenoyl chains. In this study, we have investigated the electrostatic and lateral packing properties of related phosphoglycerides and found that: 1), The dipole moment-lowering effect of the docosahexaenoyl group arises from its having a Z double bond at chain position n-3. 2), The large dipole moment-lowering effects at *sn*-1 of an ether bond to an alkyl or a 1Z alkenyl chain and that of a *sn*-2-esterified n-3 fatty acid are additive. 3), The 1Z double bond in an alkenyl chain lowers the molecular area of a phosphoglyceride and, concomitantly, makes it less compressible. 4), Ethanolamine-containing phosphoglycerides are generally less compressible than their corresponding choline analogs. Our data showing that relatively small lipid structural changes markedly alter lipid physical properties in fluid phases underscores the need to study the function of peripheral and integral membrane proteins in the presence of appropriate lipid species.

INTRODUCTION

Docosahexaenoic acid (Dh) is a major esterified component of the phosphoglycerides of retinal rod outer segments (1), primate spermatozoa (2,3), and gray matter in the brain (4,5). This is noteworthy because mammals cannot synthesize Dh de novo, but must ingest it in the diet or synthesize it from diet-derived linolenic acid. In addition, Dh must cross blood-tissue barriers to gain access to retinal rod outer segments, spermatozoa, and the brain; and there is reason to believe that the Dh that is incorporated into the membrane phosphoglycerides of the corresponding cells and tissues may influence several important functions including vision (1,6); the movement of spermatozoa (7,8); and neural development, learning and memory (9–11).

Although the mechanisms that underlie these effects remain to be clarified (12), one way to obtain clues concerning them is by studying the physical properties of different molecular species of Dh-containing phosphoglycerides (for recent reviews, see (13–15). With this possibility in mind, we recently used a standardized approach to compare the packing and electrostatic properties of homogeneous monolayers of *sn*-1-stearoyl-2-Dh (SDh) phosphoglycerides with those of homogeneous monolayers of *sn*-1-stearoyl-2-arachidonoyl phosphoglycerides (SAr), *sn*-1-stearoyl-2-oleoyl (SO) phosphoglycerides, and *sn*-1-palmitoyl-2-oleoyl phosphoglycerides (16). The results of this study identified both fatty-acyl-chain- and headgroup-dependent effects on the packing properties of the phosphoglycerides and showed (unexpectedly) that the Dh-containing phosphoglycerides had dipole moments that were substantially lower than those of comparable Ar- or O-containing diacyl phosphoglycerides. Because the dipole moment is a major determinant of the large (hundreds of millivolts) potential that exists between bulk water and the center of a bilayer membrane (17), its regulation by Dh and other determinants could be of physiological significance in electrically active membranes.

In the study described here, we expanded and refined our work on homogeneous monolayers of Dh-containing phosphoglycerides by comparing the packing and electrostatic properties of monolayers of three different groups of phosphoglycerides. One group of phosphoglycerides consisted of molecular species that contained esterified Dh in both the *sn*-1 and *sn*-2 positions (DhDh) and either phosphocholine (PC), phosphoethanolamine (PE), or phosphoserine (PS) in the *sn*-3 position. All three molecular species are found in rat retinal rod outer segment membranes (1). The second group of phosphoglycerides consisted of molecular species that contained an ether-linked, 1Z-octadecenyl (1Z-Oe) chain in the *sn*-1 position, esterified Dh or Ar in the *sn*-2 position, and esterified PC or PE in the *sn*-3 position. Similar, 1Z-Oe-Ar-PC-containing, molecular species (sometimes referred to as plasmenylcholines) appear to accumulate selectively in canine and rat myocardial sarcolemma (18,19), whereas the corresponding PE-containing phosphoglycerides (plasmenylethanolamines) are more widely distributed. The third group of phosphoglycerides consisted of molecular species that contained an ether-linked 1Z-Oe chain, an ether-linked octadecyl (Od) chain, or esterified S in the *sn*-1 position; esterified docosapentaenoic acid n-3 (Dp3) or docosapentaenoic acid n-6 (Dp6) in the *sn*-2 position, and esterified PC or PE in the *sn*-3 position. Phosphoglycerides that contain Dp6 are

Submitted April 3, 2007, and accepted for publication July 5, 2007.

Address reprint requests to H. L. Brockman, E-mail: hlbroc@hi.umn.edu.

Editor: Thomas J. McIntosh.

0006-3495/07/11/3491/13 $2.00

doi: 10.1529/biophysj.107.110072

noteworthy because they accumulate in tissues when animals ingest diets that are deficient in n-3 fatty acids (see, for example, (1)). But we focused attention on phosphoglycerides having *sn*-2-esterified Dp6 or Dp3 because the two isomers contain series of five, methylene-carbon-interrupted, Z double bonds that begin (and end) on different carbon atoms (see Results), and it seemed possible that this difference would cause the two isomers to have different electrostatic properties. Furthermore, we wanted to compare the dipole-lowering effect of the relevant, esterified isomer of Dp with that of an accompanying ether-linked alkyl chain or ether-linked 1Z-alkenyl chain.

By using the same standardized approach that we had used earlier (16) and examining several different physical properties of each phosphoglyceride, we were able to make cross comparisons of the combined data and identify key structural determinants of those physical properties. The results of these comparisons support the conclusion that *sn*-1 chain linkage to glycerol, *sn*-1 and *sn*-2 chain structures, and polar headgroups make independent contributions to the total values for most parameters. The observed importance of sometimes small structural changes on lipid physical properties emphasizes that understanding the regulation of a protein in a biological membrane requires detailed knowledge of the lipid milieu in which it functions.

MATERIALS AND METHODS

All phosphoglycerides used in the study (some custom-synthesized) were purchased from Avanti Polar Lipids (Alabaster, AL) and shipped (10 mg/ml chloroform) to the Glomset laboratory in Seattle. Phosphoglyceride names, abbreviations, and structural descriptions are listed in Table 1. The diacyl and alkylacyl phosphoglycerides were shipped in ampoules, but the alkenylacyl phosphoglycerides were shipped in amber bottles (which had not been exposed to a flame) to prevent them from being degraded. Upon arrival in the Glomset laboratory, each ampoule or bottle was opened in a glove box under argon, 0.5 mol BHT was added per 99.5 stated mol phosphoglyceride, nine volumes of hexane were added, and the phosphorus content of each solution was measured (20). Then, 0.25 ml aliquots of each solution were transferred under argon into 10, prewashed, preweighed, threaded, 0.3 ml autosampler vials (National Scientific, Lawrenceville, GA); and each vial was tightly closed with a Teflon-silicon rubber-lined cap, weighed, and then reweighed after 20 min to check for seal leakage. Lastly, those vials that showed insignificant weight loss were shipped overnight to the Brockman laboratory in Austin on gel packs that had been frozen at −20°C.

Subsequent handling of the samples, monolayer experiments, and initial data analysis were done as previously described in detail (16). Briefly, upon receipt in Austin, the vials were reweighed to identify any in which solvent loss had occurred. Of the vials that remained at their original weights, one

TABLE 1 Phosphoglycerides

Abbreviation	Chemical name
DhDhPC	1,2-di(4Z,7Z,10Z,13Z,16Z,19Z-docosahexaenoyl)-*sn*-glycero-3-phosphocholine
DhDhPE	1,2-di(4Z,7Z,10Z,13Z,16Z,19Z-docosahexaenoyl)-*sn*-glycero-3-phosphoethanolamine
DhDhPS	1,2-di(4Z,7Z,10Z,13Z,16Z,19Z-docosahexaenoyl)-*sn*-glycero-3-phosphoserine
OdDp3PC	1-O-octadecyl-2-(7Z,10Z,13Z,16Z,19Z-docosapentaenoyl)-*sn*-glycero-3-phosphocholine
OdDp3PE	1-O-octadecyl-2-(7Z,10Z,13Z,16Z,19Z-docosapentaenoyl)-*sn*-glycero-3-phosphoethanolamine
OdDp6PC	1-O-octadecyl-2-(4Z,7Z,10Z,13Z,16Z-docosapentaenoyl)-*sn*-glycero-3-phosphocholine
OdDp6PE	1-O-octadecyl-2-(4Z,7Z,10Z,13Z,16Z-docosapentaenoyl)-*sn*-glycero-3-phosphoethanolamine
OeArPC	1-O-1′-(Z)-octadecenyl-2-(5Z,8Z,11Z,14Z-eicosatetraenoyl)-*sn*-glycero-3-phosphocholine
OeArPE	1-O-1′-(Z)-octadecenyl-2-(5Z,8Z,11Z,14Z-eicosatetraenoyl)-*sn*-glycero-3-phosphoethanolamine
OeDhPC	1-O-1′-(Z)-octadecenyl-2-(4Z,7Z,10Z,13Z,16Z,19Z-docosahexaenoyl)-*sn*-glycero-3-phosphocholine
OeDhPE	1-O-1′-(Z)-octadecenyl-2-(4Z,7Z,10Z,13Z,16Z,19Z-docosahexaenoyl)-*sn*-glycero-3-phosphoethanolamine
OeDp3PC	1-O-1′-(Z)-octadecenyl-2-(7Z,10Z,13Z,16Z,19Z-docosapentaenoyl)-*sn*-glycero-3-phosphocholine
OeDp3PE	1-O-1′-(Z)-octadecenyl-2-(7Z,10Z,13Z,16Z,19Z-docosapentaenoyl)-*sn*-glycero-3-phosphoethanolamine
OeDp6PC	1-O-1′-(Z)-octadecenyl-2-(4Z,7Z,10Z,13Z,16Z-docosapentaenoyl)-*sn*-glycero-3-phosphocholine
OeDp6PE	1-O-1′-(Z)-octadecenyl-2-(4Z,7Z,10Z,13Z,16Z-docosapentaenoyl)-*sn*-glycero-3-phosphoethanolamine
OeOPC	1-O-1′-(Z)-octadecenyl-2-(9Z-octadecenoyl)-s*n*-glycero-3-phosphocholine
OeOlPE	1-O-1′-(Z)-octadecenyl-2-(9Z-octadecenoyl)-*sn*-glycero-3-phosphoethanolamine
SArPC	1-octadecanoyl-2-(5Z,8Z,11Z,14Z-eicosatetraenoyl)-*sn*-glycero-3-phosphocholine
SArPE	1-octadecanoyl-2-(5Z,8Z,11Z,14Z-eicosatetraenoyl)-*sn*-glycero-3-phosphoethanolamine
SDhPC	1-octadecanoyl-2-(4Z,7Z,10Z,13Z,16Z,19Z-docosahexaenoyl)-*sn*-glycero-3-phosphocholine
SDhPE	1-octadecanoyl-2-(4Z,7Z,10Z,13Z,16Z,19Z-docosahexaenoyl)-*sn*-glycero-3-phosphoethanolamine
SDhPS	1-octadecanoyl-2-(4Z,7Z,10Z,13Z,16Z,19Z-docosahexaenoyl)-*sn*-glycero-3-phosphoserine
SDp3PC	1-octadecanoyl-2-(7Z,10Z,13Z,16Z,19Z-docosapentaenoyl)-*sn*-glycero-3-phosphocholine
SDp3PE	1-octadecanoyl-2-(7Z,10Z,13Z,16Z,19Z-docosapentaenoyl)-*sn*-glycero-3-phosphoethanolamine
SDp6PC	1-octadecanoyl-2-(4Z,7Z,10Z,13Z,16Z-docosapentaenoyl)-*sn*-glycero-3-phosphocholine
SDp6PE	1-octadecanoyl-2-(4Z,7Z,10Z,13Z,16Z-Docosapentaenoyl)-*sn*-glycero-3-phosphoethanolamine
SOPC	1-octadecanoyl-2-(9Z-octadecenoyl)-*sn*-glycero-3-phosphocholine
SOPE	1-octadecanoyl-2-(9Z-octadecenoyl)-*sn*-glycero-3-phosphoethanolamine

Note that this table includes chemical names for the diacyl phosphoglycerides that we studied previously and, to the extent possible, uses the same abbreviations for these phosphoglycerides that we used then (16). The table also includes the chemical names of the phosphoglycerides that we studied in this investigation, but we had to change the abbreviation for docosahexaenoic acid (formerly *D*) to *Dh* to distinguish it from the abbreviation for docosapentaenoic acid (*Dp*) and for arachidonic acid (formerly *A*) to *Ar* to distinguish it from the abbreviation for molecular area. Furthermore, we used the abbreviations Dp3 and Dp6 to distinguish the n-3 and n-6 isomers of docosapentaenoic acid, *Dp*, and used the abbreviations, *Od* for octadecyl, *Oe* for 1-Z-octadecenyl, and *PC*, *PE*, and *PS* for phosphocholine, phosphoethanolamine, and phosphoserine.

vial for each species was retained for phosphate analysis to determine phosphoglyceride concentration. The remaining vials were transferred to the autosampler of an automated Langmuir film balance and, over a period of 1–2 days, a surface pressure-dipole potential-molecular area isotherm of each sample was obtained under an argon atmosphere. Before adopting this protocol, we had observed that the breakdown of highly unsaturated lipids produces a time-dependent increase in molecular area for successive samples, even when they had been stored at low temperature. Therefore, lack of dependence of replicate π-A-ΔV isotherms on time elapsed at ambient temperature before analysis was taken as evidence that the compounds studied in the current experiments remained stable. However, in the solvent used, some species of DhDh phosphoglycerides slowly formed precipitates after being brought to room temperature. Accordingly, we modified the procedure for subsequent samples of those phosphoglycerides by bringing them to ambient temperature individually, loading them into the autosampler, and analyzing them immediately. In all cases, the aqueous subphase, pH 7.4, onto which the monolayers were formed contained 5 mM HEPES sodium salt, 5 mM HEPES free acid, 0.1 M NaCl, 0.1 mM diethylenetriaminepentaacetic acid, and 1 mM $MgCl_2$. Before use, the buffer was degassed under vacuum and sparged with argon.

Representative surface pressure-molecular area (π-A) and dipole potential-lipid concentration ($\Delta V^{-1}/A$) isotherm data (*open squares*) for one of the lipids studied, DhDhPE, are shown in Fig. 1 to illustrate the analysis applied to the data. With two exceptions, 1Z-OeOPE and SOPE, all lipids studied gave similar π-A isotherms in that they lifted off from the gaseous monolayer state at near zero π into the liquid-expanded monolayer state and remained in that state until they collapsed at a π of ~47 mN/m, a value characteristic of all liquid-expanded phosphoglyceride monolayers (21). The exceptions exhibited a surface phase transition to a more condensed monolayer state below collapse. As described previously in detail, liquid-expanded π-A data can be well described by an osmotic equation of state (22),

$$\pi = (qkT/A_1)\ln[(1/f_1)[1 + A_1/(A - A_\infty)]].$$

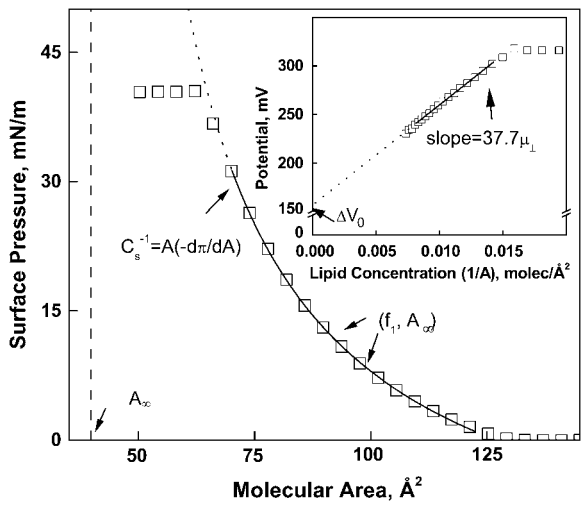

FIGURE 1 Typical liquid-expanded surface pressure-area and dipole potential-concentration isotherms showing the origin of measured and calculated descriptors. Shown are representative experimental points obtained with DhDhPE. Solid lines are obtained by fitting π-A and $\Delta V_{-1}/A$ data as described in Materials and Methods over the range of data indicated by the range of the line. Descriptors depicted are the dehydrated lipid molecular area, (A_∞); the modulus of compression, (C_s^{-1}); the lipid area-independent component of the dipole potential, (ΔV_0); and the perpendicular component of the lipid dipole moment ($\mu_\perp = [d\Delta V/d(1/A)]/37.7$).

The equation of state has three adjustable parameters, A_∞, f_1, and q, the latter two of which have been earlier shown to be correlated (23). This was verified for the lipid isotherms obtained in this study (data not shown) and, to avoid redundancy, only A_∞ and f_1 will be discussed below. As shown schematically in Fig. 1, A_∞ is the limiting molecular area when the isotherm is extrapolated to infinite π and reflects the hard-cylinder area of the lipid molecule. The activity coefficient of interfacial water at $\pi = 0$, f_1, determines the curvature of the isotherm as a function of A–A_∞ (22). To obtain f_1 and A_∞, each experimental π-A isotherm was fitted to the osmotic model from a π of 1.0 mN/m up to the pressure at which its second derivative changed sign, as indicated by the limits of the solid fit line in the figure. At a π of 35 mN/m, the molecular area of lipids in monolayers, A_{35}, corresponds to that in bilayer membranes (24,25). The value of A_{35} was determined from each isotherm for structure-function correlations. Also determined was the modulus of compression of each lipid at 35 mN/m, $C_{s35}^{-1} = A_{35}(d\pi/dA)_{35}$. This parameter, defined in Fig. 1, reflects the resistance of the film to lateral extension. For the two exceptions noted above, the proximity of the surface phase transition in the π-A isotherm to 35 mN/m necessitated calculation of A_{35} and the modulus from the fitted isotherm mathematically extrapolated to and beyond 35 mN/m.

Over the same range of molecular areas as used for π-A analysis, dipole potentials of molecules in the liquid-expanded state are generally a linear function of lipid concentration (26) as shown for DhDhPE in the inset of Fig. 1. The slope of the least-squares line through the data yields the component of the molecular dipole moment perpendicular to the interface, $\mu_\perp$, and the intercept is the area-independent potential relative to a lipid-free argon-buffer interface, ΔV_0, i.e.,

$$\Delta V = \Delta V_0 + 37.70\,\mu_\perp/A.$$

The dipole moment arises from lipid dipoles and their associated water, whereas ΔV_0 is a measure of the ability of the lipid headgroups to epitaxially order water structure in the interface over the range of packing densities that comprise the liquid-expanded monolayer state (17).

Replicate isotherms (n = 5–9) were obtained for each phosphoglyceride molecular species studied. Reported parameter values (below) are the averages of those obtained. The precision of the measurements is described by the percent standard deviations of the parameter values for each species which ranged from 0.4–1.4 for A_{35}, 0.3–3.1 for A_∞, 0.05–0.30 for f_1, 0.4–2.7 for C_{s35}^{-1}, 0.3–4.8 for ΔV_0, and 0.9–5.5 for $\mu_\perp$. Having values of a particular parameter for a number of molecular species that differ in only one structural feature, such as headgroup, *sn*-1 linkage, or *sn*-2 chain unsaturation, allows structural correlation of parameter values. To test for independence of parameter values from other structural features of the molecules, parameter values are presented below as offset plots (Results). For example, to identify *sn*-1 linkage-specific effects on the dipole moment the values obtained for *sn*-1-alkyl and -alkenyl species can be plotted against those of otherwise identical molecular species having an *sn*-1-ester linkage. In such a plot, data points that lie parallel to, but offset from, a line of identity indicate that the effects of a given structural feature on the parameter value are independent of other determinants of the value of that parameter. Inversely, points that lie on the line of identity indicate that the parameter values are independent of that structural feature.

RESULTS

Packing and electrostatic properties of DhDh phosphoglycerides

We previously showed that SDh molecular species of phosphoglycerides had dipole moments that were consistently lower than those of comparable SO or SAr molecular species. Because retinal rod outer segment membranes contain DhDhPC, DhDhPE, and DhDhPS molecular species in the range of 8–25% of each phosphoglyceride class (1), we

measured replicate surface pressure-dipole potential-molecular area (π-ΔV-A) isotherms for each of these molecular species and compared the data that we obtained with earlier data from studies of the corresponding SDh species (16). As mentioned in Materials and Methods, Fig. 1 shows a typical π-A isotherm for an homogeneous monolayer of DhDhPE. In addition, the figure identifies regions of the isotherm that point out the origin of physical parameters that were measured or calculated for each of the phosphoglycerides studied. Average values of isotherm properties and derived parameter values for the DhDh species and their corresponding SDh analogs (16) are summarized in Table 2. As shown by the values of A_{35}, the DhDh phosphoglycerides packed more loosely than the corresponding SDh phosphoglycerides. Furthermore, the monolayers became more compressible (15–25% decrease in C_{s35}^{-1}) with the additional chain unsaturation at *sn*-1, as expected. Nevertheless, as had been observed for the SDh phosphoglycerides, A_{35} of the PC-containing species remained larger than that of the corresponding PE and PS containing species, which were similar.

Table 2 also shows that the introduction of esterified Dh at *sn*-1 influenced two separate electrostatic properties of the DhDh phosphoglycerides. Thus, the dipole moments of the DhDh species were consistently lower than those of the corresponding SDh species by $\geq$100 mD, which is comparable with the dipole moment-lowering effect of *sn*-2-esterified Dh ($\sim$83 mD) when it replaces O or Ar (16). Furthermore, values of ΔV_0 (the area-independent component of the electrostatic potential) for the DhDh phosphoglycerides were 16–47 mV higher than those of the corresponding SDh phosphoglycerides, which can be compared with the respective increments of 41, 37, and 36 mV that are seen when s*n*-2-O is replaced by *sn*-2-Dh in *sn*-1-S-*sn*-2-acyl species that contain PC, PE, or PS (16).

Packing and electrostatic properties of docosahexaenoic acid-containing alkenylacyl phosphoglycerides

This set of experiments examined homogeneous monolayers of phosphoglycerides that contained an *sn*-1-ether-linked 1Z-Oe chain; *sn*-2-esterified Dh, Ar, or O; and PC or PE. Table 3 compares the average values that we obtained for the isotherm properties and derived parameter values of these phosphoglycerides with the values that we previously obtained for the corresponding SDh, SAr, and SO molecular species (16). As the table shows, the packing properties of the 1Z-OeDh-, 1Z-OeAr-, and 1Z-OeO-phosphoglycerides resembled those of the corresponding S-acyl phosphoglycerides. But the dipole moments of the 1Z-Oe-acyl phosphoglycerides were much lower than those of the comparable diacyl phosphoglycerides, and *sn*-2-esterified Dh had relatively large dipole-lowering effects on the 1Z-Oe-acyl phosphoglycerides. Nevertheless, it is noteworthy that the absolute values of these effects were very similar to each other and that $\mu_\perp$ was lowered by an average of 87 $\pm$ 15 mD. These and other of the results shown in the table will be discussed further in the context of comparisons of a larger group of phosphoglyceride molecular species (see below).

Packing and electrostatic properties of Dp-containing phosphoglycerides

Having shown that Dh has a consistent $\mu_\perp$-lowering effect on phosphoglycerides (Tables 2 and 3 and (16)), we sought to explore its basis. It seemed possible that it might depend on the 4Z-double bond in Dh, which is located close to the *sn*-2-glyceryl ester regions of these phosphoglycerides. This is because previous studies had provided evidence that the $\mu_\perp$ values of phosphoglycerides are determined primarily by such regions and their associated water molecules (17) and because the presence of the 4–5 double bond in the sphingosine base of ceramides has a pronounced effect on its measured dipole potential (27). But our findings with regard to the $\mu_\perp$-lowering effects of esterified Dh were based on comparisons with molecular species in which the esterified Dh replaced *sn*-1-esterified S or *sn*-2-esterified Ar or O; and these three fatty acids differ from Dh not only in double bond position, but also in double bond number and carbon number. Therefore, we decided to do a more closely matched set of experiments using homogeneous monolayers of phosphoglycerides that contained either *sn*-2-esterified Dp3 or *sn*-2-esterified Dp6. (These two fatty acids have the same number of carbons as Dh but five, rather than six,

TABLE 2 Comparison of *sn*-1-stearoyl and *sn*-1-docosahexaenonyl phosphoglycerides

Lipid Abbreviation	Isotherm replicates	A_{35} Å^2	A_∞ Å^2	f_1	C_{s35}^{-1} mN/m	ΔV_0 mV	ΔV_0(SDh) - ΔV_0(DhDh) mV	$\mu_\perp$ mD	$\mu_\perp$(SDh) - $\mu_\perp$(DhDh) mD	Total ΔV_{35} mV	Net change $\Delta\Delta V35$ mV
SDhPC	*	64.0	39.7	1.125	116	153	−16	431	106	407.6	64
DhDhPC	8	70.5	41.4	1.104	98	169		325		343.2	
SDhPE	*	57.4	39.6	1.151	126	117	−38	431	154	400.5	90
DhDhPE	8	67.2	40.2	1.112	94	155		277		310.5	
SDhPS	*	56.0	37.6	1.138	119	25	−47	387	100	285.5	51
DhDhPS	7	66.8	41.6	1.103	93	72		287		234.5	
Average (SD)							34(±16)		120(±30)		68(±20)

*Previous study.

TABLE 3 Comparison of *sn*-1-octadecanoyl-*sn*-2-acyl and *sn*-1-octadecenyl-*sn*-2-acyl phosphoglycerides

Lipid abbreviation	Isotherm replicates	A_{35} Å^2	A_∞ Å^2	f_1	C_{s35}^{-1}mN/m	ΔV_0 mV	ΔV_0(X) - ΔV_0(Dh) mV	$\mu_\perp$ mD	$\mu_\perp$(X) - $\mu_\perp$(Dh) mD	ΔV_{35}	$\Delta\Delta V35$
OeOPE	7	51.7	44.5	1.257	209	103	−33	207	97	253.9	42
OeArPE	6	55.2	42.2	1.193	156	101	−35	219	110	251.1	39
OeDhPE	7	54.1	40.3	1.176	142	136		110		212.1	—
OeOPC	6	54.4	40.7	1.188	145	111	−47	262	81	292.3	25
OeArPC	8	58.2	39.7	1.156	130	117	−41	262	82	287.3	20
OeDhPC	6	62.4	41.0	1.134	126	158		181		267.5	—
SOPE	*	53.3	42.7	1.201	180	80	−37	521	90	448.6	48
SArPE	*	56.4	40.5	1.167	138	86	−31	505	74	423.3	23
SDhPE	*	57.4	39.6	1.151	126	117		431		400.5	—
SOPC	*	58.0	39.3	1.155	128	112	−42	494	63	432.8	25
SArPC	*	63.6	40.3	1.135	124	121	−32	528	97	434.3	27
SDhPC	*	64.0	39.7	1.125	116	153		431		407.6	—
Average (SD)							−37 (±6)		87 (±15)		31 (±10)

*Previous study.

methylene-interrupted Z double bonds, which respectively begin at carbon 4 or 7 and end at carbon 16 or 19 for Dp6 and Dp3.) Moreover, we studied the properties of six different pairs of phosphoglycerides (Table 4) to compare the effects of the two *sn*-2-esterified Dp isomers with those of *sn*-1-ether-linked Od chains, *sn*-1-ether-linked 1Z-Oe chains, and *sn*-3 linked PE or PC groups.

The results of these experiments showed that the $\mu_\perp$ values of those phosphoglycerides that contained *sn*-2-esterified Dp3 were consistently lower than those of corresponding phosphoglycerides that contained *sn*-2-esterified Dp6. Thus, although the $\mu_\perp$ values of the phosphoglycerides varied over a range of 300 mD (Table 4), Fig. 2 shows graphically that there is an essentially constant offset of 81 ± 4 mD between the six pairs of otherwise identical Dp3 and Dp6 species. Both the direction and value of this offset are similar to the $\mu_\perp$-lowering effect of esterified Dh relative to diacyl and 1Z-Oe-acyl phosphoglycerides that otherwise differ only in having Ar or O rather than Dh at *sn*-2, 87 ± 15 mD (Table 3). Therefore, it is very unlikely that the 4Z double bond of *sn*-2-esterified Dh is responsible for its $\mu_\perp$-lowering effect (recall the first double bond of Dp3 occurs at carbon 7 rather than carbon 4). Instead, for both Dp3 and Dh these effects appear to depend on the 19Z (i.e., n-3) double bond. It should be noted that the three or four Z double bonds within the set of five or six for Dh or Dp3 would be expected to make little contribution to $\mu_\perp$ because they are distal from both ends of the chain and exist in a nearly uniform dielectric environment. Thus, overall, the data in Tables 2–4 and Fig. 2 show that: 1), the presence of Dh or Dp3 at either *sn*-1 or *sn*-2 of phosphoglycerides causes a >80 mD decrement in their dipole moments, relative to the dipole moments of corresponding phosphoglycerides that contain n-6 and n-9 acyl groups at *sn*-2; 2), this change is independent of phosphoglyceride headgroup or the nature of the linkage at *sn*-1; and 3), each esterified Dh or Dp3 increases ΔV_0 by 25–30 mV. Moreover, the data in Table 4 show that: 1), for molecular species of phosphoglycerides that have the same headgroup, the effects of *sn*-2-esterified Dp3 on $\mu_\perp$ are additive to those of an *sn*-1-ether-linked Od chain or 1Z-Oe chain; 2), as observed previously for 1Z-OeDh phosphoglycerides (Table 3), values of $\mu_\perp$ for 1Z-OeDp3 phosphoglycerides that contain PE are lower than those of corresponding phosphoglycerides that contain PC;

TABLE 4 Comparison of docosapentaenoic acid n-3 and docosapentaenoic acid n-6 phosphoglycerides

Lipid abbreviation	Isotherm replicates	A_{35} Å^2	A_∞ Å^2	f_1	C_{s35}^{-1} mN/m	ΔV_0 mV	$\mu_\perp$ mD
OdDp3PC	7	64.8	41.4	1.1211	122	171	260
OdDp6PC	6	63. 5	38.4	1.1237	119	146	346
OdDp3PE	7	57.8	41.0	1.1487	137	149	266
OdDp6PE	7	56.7	38.4	1.1478	129	121	346
OeDp3PC	7	62.8	42.3	1.1370	133	162	156
OeDp6PC	8	59.1	39.0	1.1462	127	135	232
OeDp3PE	6	55.5	42.3	1.1796	152	145	90
OeDp6PE	7	56.4	42.0	1.1740	150	119	174
SDp3PC	6	64.8	40.3	1.1229	117	156	380
SDp6PC	6	63.0	38.3	1.1283	115	129	459
SDp3PE	6	57.1	40.3	1.1543	135	128	373
SDp6PE	5	55.5	38.3	1.1560	131	98	450

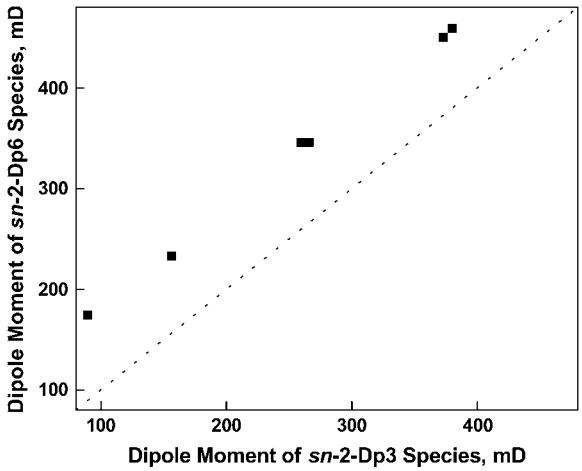

FIGURE 2 Effect of Z double bond position on the dipole moment of otherwise identical *sn*-2-docosapentaenoyl phosphoglyceride molecular species. The Z-double bond closest to the chain terminal carbon (*n*) was either n-3 (Dp3) or n-6 (Dp6). The dotted line is a line of identity (intercept = 0, slope = 1). Data are from Table 4.

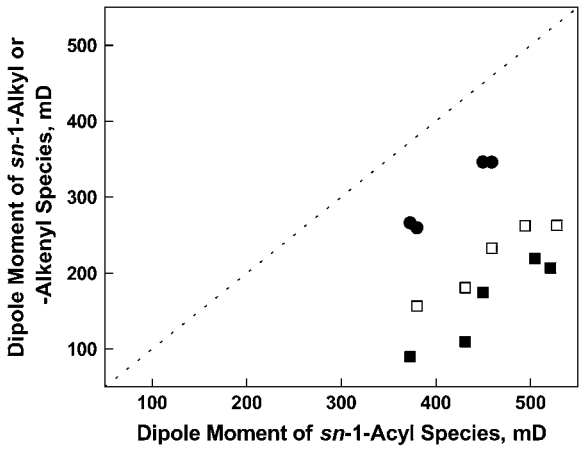

FIGURE 3 Effect of the linkage of the 18-carbon *sn*-1 substituent on the dipole moment of otherwise identical phosphoglyceride molecular species. Values of $\mu_\perp$ for alkyl ether (*sn*-1-Od) PCs and PEs (●) and alkenyl ether (*sn*-1-Oe) species of PEs (■) and PCs (□) are plotted against those of the corresponding ester (*sn*-1-S) species. The dotted line is a line of identity (intercept = 0, slope = 1). Data are from Tables 3 and 4.

and 3), a similar type of headgroup dependency exists for 1Z-OeDp6 phosphoglycerides, but not for OdDp3 or OdDp6 phosphoglycerides.

Structural determinants of the properties of phosphoglycerides revealed by cross comparisons of the data

Because we had used the same standardized approach to study the packing and electrostatic properties of homogeneous monolayers of the phosphoglycerides that are shown in Tables 3 and 4, i.e., those with 18-carbon chains at *sn*-1, it became possible to perform cross comparisons of the data to help identify structural features that influenced their properties. As described in Materials and Methods and exemplified for Dp3-containing species in Fig. 2, we tested for the simplest form of structural dependence, a constant difference, between pairs of species that, but for one structural feature, were identical.

Effect of sn-1 linkage on the electrostatic properties of phosphoglycerides

Fig. 2 (above) shows that the position of double bonds in the Dp3 and Dp6-containing phosphoglycerides alters $\mu_\perp$ in a manner that is independent of headgroup or *sn*-1 linkage. Fig. 3 shows the influence of *sn*-1 linkage not just for the Dp-containing species but for all 14 comparable pairs of compounds listed in Table 1 (note that the parameter values of the compounds are summarized in Tables 3 and 4). The members of each pair are identical except for the linkage of the 18-carbon *sn*-1 chain and include species with Dh, Dp3, Ar, or O esterified at *sn*-2. The $\mu_\perp$ values of the Od-acyl PEs and PCs (*solid circles*) are lowered similarly to those of the comparable diacyl species (111 ± 7 mD, Fig. 3). In contrast, those of the 1Z-Oe-acyl species are lowered more than twice as much as the Od-acyl species but, importantly, in a headgroup-dependent manner. Specifically, Fig. 3 shows that the $\mu_\perp$ values of the 1Z-Oe-acyl-PCs (*open squares*) and 1Z-Oe-acyl-PEs (*solid squares*) average 240 ± 18 mD and 295 ± 22 mD, respectively, below the line of identity representing the corresponding diacyl species. Note that for the PEs, this is a decrease in $\mu_\perp$ relative to the diacyl species of 60–75%! Direct comparison of species with like *sn*-1 linkages on the basis of headgroups (graph not shown) indicates that the $\mu_\perp$ values of Od-acyl and diacyl species are identical, but that those of 1Z-Oe-acyl-PEs are lower by 59 ± 11 mD relative to comparable 1Z-Oe-acyl-PCs. This, together with the data in Tables 3 and 4 and Fig. 3, suggests some interdependence between at least one of the headgroups at *sn*-3 and the 1Z-Oe linkage at *sn*-1.

Supporting the notion of interplay between the headgroup and *sn*-1 linkage is the observation that ΔV_0 is essentially unchanged when 1Z-Oe-acyl PCs replace diacyl PCs (Fig. 4, *solid squares*), but is increased 19 ± 3 mV when an Od-acyl PE or PC or a 1Z-Oe-acyl PE replaces its diacyl analog (*open circles*). Moreover, relative to PCs, ΔV_0 values for 1Z-Oe-acyl PE species are lowered only half as much as those of diacyl PEs (15 ± 5 vs. 33 ± 3 mV, graph not shown). Independently of these effects, ΔV_0 is also raised 27 ± 2 mV (graph not shown) by n-3 as compared with n-6 unsaturation in the Dp-containing species. The comparison of electrostatic data suggests, overall, that the presence of the 1Z-Oe linkage at *sn*-1 in a PE species changes interfacial orientation, conformation, or hydration in a manner distinct from its effects on PC species.

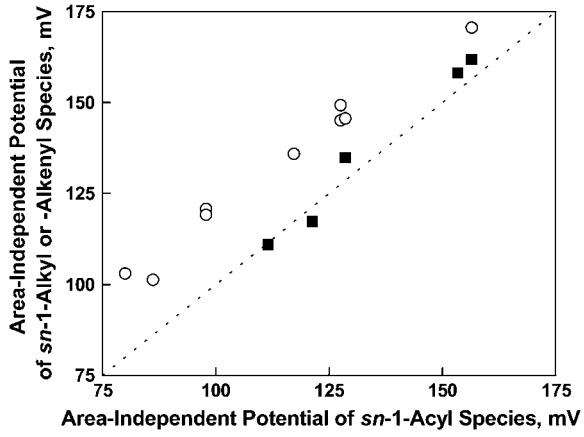

FIGURE 4 Effect of the linkage of the 18-carbon *sn*-1 substituent on the area-independent potential of otherwise identical phosphoglyceride molecular species. Values of ΔV_0 for alkenyl ether (*sn*-1-Oe) species of PCs (■) and alkenyl ether (*sn*-1-Oe) species of PEs plus alkyl ether species of PEs and PCs (○) are plotted against those of the corresponding ester (*sn*-1-S) species. The dotted line is a line of identity (intercept = 0, slope = 1). Data are from Tables 3 and 4.

Effect of Od and 1Z-Oe groups on the molecular areas of phosphoglycerides

Initial comparisons of the packing properties of alkenylacyl phosphoglycerides that contained esterified Dh or Ar with those of corresponding diacyl phosphoglycerides provided evidence that the molecular areas of the alkenylacyl phosphoglycerides at 35 mN/m, A_{35}, were somewhat lower than those of corresponding diacyl phosphoglycerides (Table 3). Moreover, subsequent comparisons of 1Z-Oe-acyl phosphoglycerides that contained esterified Dp3 or Dp6 with corresponding diacyl phosphoglycerides yielded similar results (Table 4); and when the data from the two types of comparisons were combined and analyzed, it became apparent that the different types of 1Z-Oe-acyl phosphoglycerides had A_{35} values that were generally, but not consistently (1.2–5.5 Å^2), lower than those of corresponding diacyl phosphoglyceride molecular species. But the significance of this fact did not become apparent until the data for the Dp-containing Od-acyl phosphoglycerides were included in the comparisons (Table 4). The areas of the Od-acyl phosphoglycerides were found to be larger than those of the corresponding 1Z-Oe-acyl phosphoglycerides and essentially equal to those of the corresponding diacyl phosphoglycerides. This indicates that the 1Z double bonds in the *sn*-1-Oe chains, rather than the *sn*-1-ether bonds to these chains, control the packing properties of 1Z-Oe-acyl phosphoglycerides. It also suggests that the carbonyl group of the *sn*-1-acyl species does not contribute to the areas of these *sn*-2 highly unsaturated species at membrane-relevant π-values.

The lipid molecular area at a particular surface pressure reflects in part the intrinsic hard cylinder area of the molecule, A_∞, which is obtained by mathematically extrapolating the π-A isotherm to infinite π (Fig. 1). Effectively, A_∞ is the cross-sectional area of the dehydrated lipid in the interfacial plane. Comparisons of the values of this parameter for the different molecular species of phosphoglycerides showed that they were complex functions of the substituents of the phosphoglycerides. The A_∞ values of those phosphoglycerides that contained *sn*-2-esterified Dp3 were on average 2.2 ± 1.1 Å^2 larger than the A_∞ values of their Dp6 counterparts (graph not shown). On the other hand, for all pairs of PC- or PE-containing species having either of the n-3 acyl groups (Dh or Dp3) at *sn*-2, A_∞ of the PC-containing species was identical (within error) to that of the equivalent PE-containing species (Fig. 5, *solid squares*); and the same was true for the n-6-containing pairs of PC- or PE-containing species (*solid circles*) unless the *sn*-1 linkage was 1-Z-Oe (*open circles*). Nor was identity observed between the A_∞ values of PC- and PE-containing species having either an S or 1Z-Oe linkage at *sn*-1 and O (n-9) at *sn*-2 (*open triangles*). For these four pairs of species, which deviated from the line of identity, the A_∞ of species that contained PE was larger by 2–4 Å^2 than that of species that contained PC, the opposite of what was observed for hydrated areas, e.g., A_{35} (Tables 3 and 4 and (16)). The deviations may simply reflect scatter in values for this extrapolated parameter, but there is structural consistency to them. (The significance of this value rests on the assumption that the only change that occurs as a function of infinite pressure is a loss of water molecules that are bound to the polar headgroups of phosphoglycerides. This caveat should be kept in mind because changes in polar headgroup orientation have been noted under other circumstances (28–30).)

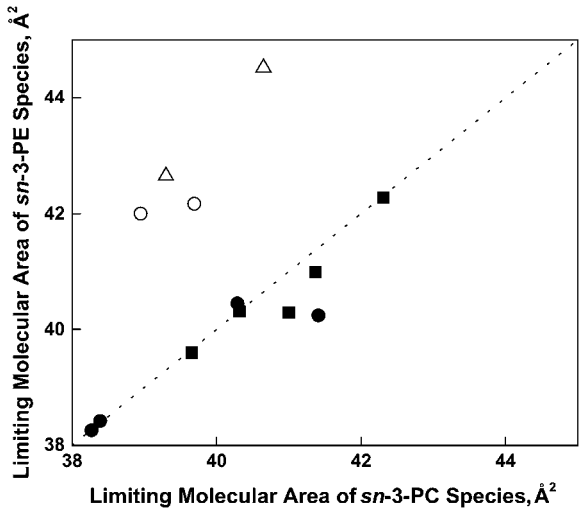

FIGURE 5 Effect of the *sn*-3 phosphoglyceride headgroup on the limiting molecular area of otherwise identical phosphoglyceride species. Values of A_∞ for PE species having an n-3 acyl chain at *sn*-2 (■), n-6 *sn*-2-acyl chain and *sn*-1-S or *sn*-1-Od (●), n-6 *sn*-2-acyl chain and *sn*-1-Od (○), and n-9 *sn*-2-acyl chain and *sn*-1-S or -Oe (Δ) are plotted against those of the corresponding PC species. The dotted line is a line of identity (intercept = 0, slope = 1). Data are from Tables 2–4.

In the osmotic view of the gas-liquid interface the surface pressure of lipid monolayers is determined by the interfacial area occupied by water, i.e., A_π-A_∞. This dependence appears not only in the equation of state we employ but also in others (23). To determine how this quantity is regulated by lipid structure near the interface with bulk water, values of A_{35}-A_∞ were compared on the basis of *sn*-1 linkage (Fig. 6). The figure shows that the A_{35}-A_∞ values of all 1Z-Oe-acyl species (*solid squares*) were on average smaller than their diacyl counterparts by 3.8 ± 0.8 Å^2. In contrast, the Od-acyl species (*open circles*) remained unchanged relative to the diacyl species, as shown by their proximity to the line of identity. Thus, the 1Z double bond at *sn*-1 appears to consistently reduce the hydrated area of the interface. In another test, the data were paired with respect to the phosphoglyceride headgroup (graph not shown). In this case, A_{35}-A_∞ values of PC-containing phosphoglycerides were uniformly larger than those of the corresponding PE-containing phosphoglycerides by 6.9 ± 0.8 Å^2, independent of both *sn*-1 linkage and acyl structure. Lastly, comparison of the A_{35}-A_∞ values of Dp3 and Dp6 species showed n-6 values to be only 0.8 ± 0.7 Å^2 larger, which approximates the limit of error of area measurements. This suggests that the primary, albeit small, effect of n-3 vs. n-6 unsaturation on A_{35} arises from the effect of n-3 unsaturation on the close-packed areas of the molecules. Overall, the consistency of the A_{35}-A_∞ offsets with changes in structure shows that each structural difference between molecules is an essentially independent determinant of the hydrated molecular area. This implies that, at least in part, the *sn*-1 linkage, chain unsaturation, and headgroup compete laterally for the same space in the interface.

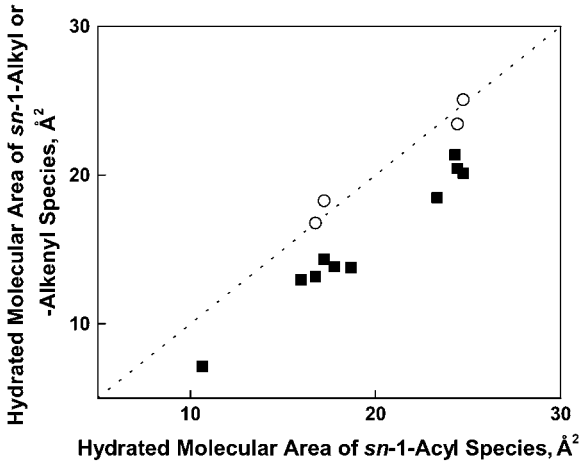

FIGURE 6 Effect of the linkage of the 18-carbon *sn*-1 substituent on the hydrated area at 35 mN/m of otherwise identical phosphoglyceride molecular species. Values of A_{35}-A_∞ for species having either an ether (*sn*-1-Od) (○) or vinyl ether (*sn*-1-Oe) (■) linkage are plotted against those of the corresponding acyl (*sn*-1-S) species. The dotted line is a line of identity (intercept = 0, slope = 1). Data are from Tables 3 and 4.

Structural determinants of monolayer compressibility

The lateral elasticity of lipid layers is an important regulator of the partitioning of soluble proteins to interfaces, the lateral distribution of proteins in the membrane plane in phase-separated systems, and the functioning of membrane channels and pores (31,32). Following bilayer convention, elasticity/compressibility is usually expressed as its reciprocal and normalized for lipid area, i.e., the modulus of compression, C_s^{-1} (see Fig. 1). As noted in Materials and Methods, evaluation is typically carried out at the membrane-relevant π of 35 mN/m and values of C_{s35}^{-1} are given in Tables 2–4. Unlike most of the other parameters compared by structural features above, C_{s35}^{-1} did not show a simple offset dependence on *sn*-1 linkage for the 1Z-Oe-acyl species as compared with their diacyl counterparts. Rather, the dependence is more linear (graph not shown) and least-squares analysis ($R^2 = 0.98$) of the results gives a slope of 1.5 with an intercept of −53 mN/m. This means that, in the range of values obtained, the vinyl ether is less compressible, presumably as a consequence of the 1Z-Oe-acyl species having smaller values of A_{35}-A_∞ (Fig. 6). In contrast, the values for the Od-acyl species appeared identical to those of the corresponding diacyl species, though the range of this comparison is limited. A linear relationship was also observed when C_{s35}^{-1} data were plotted to compare the effects of headgroup (Fig. 7, $R^2 = 0.86$, slope = 2.5, intercept = −166 mN/m). This indicates that the PC-containing phosphoglycerides were generally more compressible than their PE-containing counterparts with much larger differences between comparable species that contained PC or PE associated with less chain unsaturation at *sn*-2. Also shown in Fig. 7, but not included in the linear fit, is a point (*solid triangle*) representing the data for DhDh PC and PE from Table 2. For these highly unsaturated species the moduli were essentially identical, but also near the extrapolation of the line fitted to the data from species with 18 carbons at *sn*-1. In contrast to these dependencies, comparison of C_{s35}^{-1} values on the basis of n-3 vs. n-6 unsaturation for the Dp-containing species (not shown) indicated that n-3 unsaturation lowered C_{s35}^{-1} by only 4 ± 2 mN/m or ~3%.

DISCUSSION

Electrostatic properties of polyunsaturated phosphoglycerides

We showed earlier that pairs of phosphoglyceride molecular species which differed only in having either Dh or Ar esterified at the *sn*-2 position of glycerol had nearly identical A_{35} and C_{s35}^{-1} values in monolayers. Despite these similarities and the fact that both *sn*-2-acyl groups were highly unsaturated, the comparable species exhibited different $\mu_\perp$ values. Moreover, that difference was consistent in that the $\mu_\perp$ values of Dh-containing species were ~87 mD lower than those of their Ar-containing counterparts. Primary goals of this work

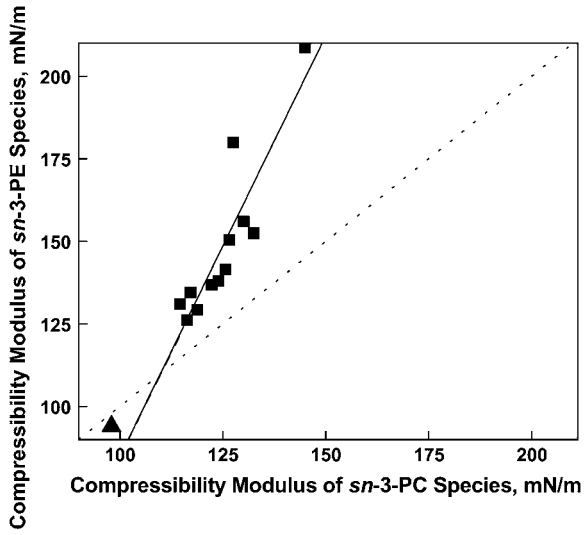

FIGURE 7 Effect of the *sn*-3 phosphoglyceride headgroup on the modulus of compression at 35 mN/m of otherwise identical phosphoglyceride species. Values of C_{s35}^{-1} for PE species are plotted against those of corresponding PC species for phosphoglycerides having an 18-carbon substituent (S, Od, or Od; ■) or Dh (▲) at *sn*-1. The dotted line is a line of identity (intercept = 0, slope = 1). Data are from Tables 2–4.

were: 1), to compare this effect with that of *sn*-1-esterified Dh; 2), to compare it with that of the *sn*-1-ether-linked 1Z-Oe chain; 3), to determine the origin of the $\mu_\perp$-lowering effect of *sn*-2-Dh by comparing the properties of phosphoglycerides that contain *sn*-2-esterified isomers of Dp; and 4), to compare the effects of *sn*-2-esterified Dp with those of *sn*-1-esterified S, an *sn*-1-ether-linked Od chain, or an *sn*-1-ether-linked 1Z-Oe chain. As reported above, replacement of *sn*-1-S by Dh to form DhDh phosphoglycerides (DhDhPC, DhDhPE, or DhDhPS; Table 2) caused an additional lowering of $\mu_\perp$ that was similar to that caused by the introduction of the first Dh at *sn*-2 in place of Ar or O (Table 3). The Dh effect at *sn*-2 was also retained if the linkage at *sn*-1 was 1Z-Oe, rather than S, even though the linkage change independently lowered $\mu_\perp$ by a large amount (Table 3). Overall, these structural changes showed that each esterified Dh chain was an essentially independent determinant of $\mu_\perp$, lowering it by $\geq$80 mD relative to other acyl groups. A similar effect was observed in studies of phosphoglycerides that contained *sn*-2-esterified Dp3, but not in those that contained *sn*-2-esterified Dp6, leading to the conclusion that it is the 19Z (n-3) double bond, common to Dh and Dp3, that lowers $\mu_\perp$ (Table 4).

The terminal methyl group of a lipid chain can potentially contribute as much as 665 mD to $\mu_\perp$ of a lipid molecule in a monolayer if the chain is fully extended perpendicular to the lipid-water interface (33). Simple electrostatic calculations (Molecular Modeling Pro Ver. 3.2, ChemSW, Fairfield, CA) indicate that adding a 19Z (n-3) double bond to Dp6 to create Dh does not significantly change the contribution of the methyl group to $\mu_\perp$ if chain area in the interfacial plane is kept minimized. However, an NMR-based comparison of the electron densities and conformational flexibilities of SDhPC and SDp6PC showed that in these polyunsaturated species, the presence of the additional 19Z (n-3) double bond in Dh yields faster reorientational dynamics and increases the relative electron density of the Dh chain nearer the headgroup region of the molecule (34). Because the contribution of the terminal methyl group to the dipole moment is vectorial, the increased conformational freedom could reasonably increase the time-averaged angle of the methyl group dipole moment of the n-3 species relative to the interfacial normal, more than for the n-6 species and, thereby, lower its contribution to $\mu_\perp$.

The lipid concentration-dependent component of the measured dipole potential at, for example, $\pi = 35$ mN/m can be calculated as 37.7 $\mu_\perp/A_{35}$. For the pairs of species that are identical except for having S or Dh at *sn*-1 (Table 2), Ar or Dh at *sn*-2 (Table 3), or Dp6 or Dp3 at *sn*-2 (Table 4), the values of this contribution are 53–128 mV lower for the n-3 (Dh or Dp3) species. However, the net decrements in the measured dipole potential, ΔV_{35} are smaller, ranging from 25 to 90 mV lower for the n-3 species. The smaller decrements for the ΔV_{35} arise from compensatory changes in the lipid concentration-independent contribution to the measured potential, ΔV_0. For bilayers, lipid structure-dependent changes in this potential component, readily measured in monolayers, are experimentally inaccessible (17). This inaccessibility does not imply, however, that changes in ΔV_0 are unimportant. Recent data suggests that the properties of interfacial water regulate soluble protein interaction with the interface (35). One way the presence of a n-3 double bond could affect a water structure-related parameter like ΔV_0 more than a saturated chain or one having an n-6 or n-9 double bond is suggested by the study noted above (34), which speculated that the higher interfacial electron density of Dh in SDhPC relative to Dp6 in SDp6PC could arise from increased interaction of the n-3 double bond of SDhPC with interfacial water.

Alternatively, could the compensatory changes in the lipid concentration-independent ΔV_0 be influenced by the magnitude of the lipid-water concentration-dependent net dipole moment, $\mu_\perp$? To explore that possibility, we plotted ΔV_0 as a function of $\mu_\perp$ (Fig. 8) for not only each species reported in Tables 2–4 in this study but also for the additional PE-, PC-, and PS-containing species reported earlier (16). The figure shows that if the data are combined into sets on the basis of *sn*-3 substituent and *sn*-1 linkage (*sn*-1 alkyl and acyl, but not alkenyl, species are combined), ΔV_0 is a reasonably linear ($R \geq 0.92$) function of $\mu_\perp$ for each set. The vertical offsets between the lines are consistent with the postulated epitaxial effects of different lipid headgroups on interfacial water postulated earlier as contributors to ΔV_0 (17). The behavior shown in Fig. 8 refines this concept such that the headgroup contribution of ΔV_0 should be given by the intercepts of the lines. Conceptually, each intercept is the potential difference between an argon-water interface and a comparable interface

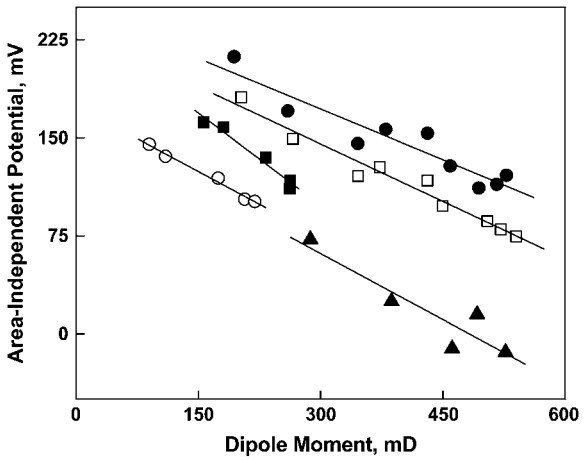

FIGURE 8 Effect of the dipole moment of a phosphoglyceride species on its lipid area-independent dipole potential. Values of ΔV_0 for PCs having an *sn*-1ester or ether (S, Dh, Od; ●), PCs having an *sn*-1 alkenyl ether (Oe, ■), PEs having an *sn*-1 ester or ether (S, Dh, Od; □), PEs having an *sn*-1 alkenyl ether (Oe, ○) or PSs having an *sn*-1 ester (S, Dh; ▲) are plotted against the $\mu_\perp$ of the same species. The solid lines are least-squares fit lines through each data set. Data are from Tables 2–4 and (16).

in which water between lipids is organized by a lipid headgroup. For the two groups of lipids with phosphocholine at *sn*-3 the intercepts of the lines are approximately equal at 240 and 250 mV, whereas the values for the ether or ester PEs and vinyl ether PEs are different, 233 and 174 mV. The linearity of each group of data shown in Fig. 8 and the similar (−2.6 to −4.7 mV/mD) slopes of the least-squares lines among groups show that in addition to the reorganization of vicinal water molecules by lipid dipoles to produce the net $\mu_\perp$, e.g., (36), there is a secondary, proportional, lipid-concentration-independent effect of the net value of $\mu_\perp$ on ΔV_0. It should be noted, however, that the lateral concentration of a fluid lipid in the liquid-expanded state is very high in that roughly 1/4–1/2 of the area of the interface is occupied by lipid (compare A_{35} values with A_∞ in Tables 2–4) and lipid molecular area changes only approximately twofold between liftoff and collapse of a typical π-*A* isotherm (e.g., Fig. 1). Thus, this secondary effect may simply appear linear over the short range of molecular separations reflected in the isotherms. In any event, Fig. 8 shows that the presence of lipid dipoles in an interface, like headgroups, affect the properties of interfacial water molecules that may not be directly associated with the lipids. Overall, the behavior shown in Fig. 8, which arises from lipid chains having no, n-3, n-6, and n-9 unsaturation, suggests strongly that the compensation between the potentials arising from $\mu_\perp$ and from ΔV_0 observed between n-3 and other chains does not arise from any unique interaction of the n-3 double bond with interfacial water but simply reflects a more general dependence of ΔV_0 on $\mu_\perp$ (Fig. 8).

Our studies of the electrostatic properties of phosphoglycerides showed, for the most part, that the effects of an ether bond to an *sn*-1 Od or Oe chain, a 1Z double bond in an Oe chain, 19Z unsaturation at *sn*-2, and polar headgroups were additive. However, we did observe an interrelationship between headgroup and the 1Z-Oe linkage at *sn*-1 for the dipole moment that appears to be associated with 1Z-Oe-acyl PE molecular species as compared to corresponding PC species (Fig. 3) and this PE/PC difference with respect to *sn*-1 linkage can also be seen in Fig. 8. Specifically, the PC-containing sets share a common intercept whereas the PE-containing sets do not. Although alkenylacyl lipids have glycerol conformations in which the *sn*-1 and *sn*-2 chains are more equivalent than in diacyl or dialkyl lipids, the conformations are not distinctly different for alkenylacyl species that contain PC or PE (reviewed in (37)), at least for the *sn*-2-O species compared. This raises the possibility that for the polyunsaturated species described here the conformations may differ, possibly as a consequence of differences in intermolecular hydration and hydrogen bonding involving ethanolamine and the 1Z double bond of the alkenyl species. Alternatively, rotation of the 2–3 carbon-carbon bond of the *sn*-1-chain might allow this chain to pack more effectively with the *sn*-2-Dh if the latter tends to have an angle iron-shaped conformation (38).

The dipole potential of monolayers exists between the aqueous phase adjacent to water of hydration of phosphoglyceride headgroups and the ends of the lipid chains. In bilayers it exists between the aqueous phase and the center of the membrane for each leaflet. Previous studies have shown correspondence between the dipole potentials of bilayer membranes and those of monolayers at comparable lipid packing density (17,39). Lower dipole potentials for ether lipids in bilayers, relative to ester lipids, have also been reported in monolayers (40) and bilayers (41). Thus, it can be expected that the difference between n-3 and n-6 dipole moments documented in this study will regulate the dipole potential of bilayers in which these lipids are present. Less widely recognized are the differences between lipids in ΔV_0 values, as shown in this work. This is perhaps because ΔV_0 cannot be measured in bilayers. Differences in ΔV_0 values among lipid species reflect differences in the organization of water near lipid headgroups. The structure of this water likely influences the interactions of proteins and other solutes with bilayer membranes.

Packing properties of highly unsaturated phosphoglycerides

In our earlier study of diacyl phosphoglyceride species we observed, unexpectedly, that even though *sn*-1-acyl chain length and *sn*-2-acyl chain unsaturation regulated molecular area, the A_{35} values of species that contained PC were independently larger by 7.1 Å^2 than those of fatty-acyl-chain-equivalent species that contained other polar headgroups (16). This suggested that headgroups and chains compete in some way for interfacial area. In this study of additional phosphoglyceride molecular species, including

sn-1-Od- and *sn*-1-1Z-Oe- species, the trend was maintained with A_{35} values of species that contained PC averaging 6.0 ± 2.1 Å^2 larger than comparable, PE-containing species. When this comparison was made using A_{35}-A_∞ the difference was 6.9 ± 0.8 Å^2, showing that the effect primarily reflects differences in the hydrated interfacial areas associated with the lipids. Even when Dh was esterified at both *sn*-1 and *sn*-2, the effect persisted with DhDhPC being 3.3 and 3.7 Å^2 larger than comparable species that contained PE or PS. This occurred despite the fact that the DhDh species were 6.5–10.8 Å^2 larger than their SDh counterparts (Table 1), supporting the previous conclusion (16) that acyl chains compete with the PC headgroup for interfacial occupancy.

In a study of semisynthetic diacyl, alkyl-acyl, and alkenyl-acyl PC and PE species, which was done many years ago, similar, but not identical, trends in molecular areas were noted (40). However, in that study the fatty acyl compositions at *sn*-1 and in some cases *sn*-2 differed within each series and some branched chains were present. This makes comparison with our study difficult. In this study, pure *sn*-1-Od-*sn*-2-acyl species having *sn*-2-esterified isomers of Dp exhibited areas identical to those of their *sn*-1-S-*sn*-2-acyl counterparts. In contrast, the *sn*-1Z-Oe-2-acyl species in the same series were smaller than the corresponding *sn*-1-Od-2-acyl and *sn*-1-S-2-acyl species, and uniformly so (3.8 ± 0.8 Å^2) when compared on the basis of A_{35}-A_∞. Interestingly, this value is equal but opposite to the average increase in A_{35} observed when Ar or Dh replaces O at *sn*-2 in similar diacyl lipids (16), suggesting that, on average, an alkenyl-acyl species having a highly unsaturated *sn*-2-acyl chain will pack with approximately the same molecular area as a comparable diacyl species having O at *sn*-2.

The modulus of compression of monolayers and bilayers linearly controls the free energy of partitioning of peripheral proteins to membranes and, hence, is a biologically important mechanical property (31,32). The value of the modulus is strongly determined by the hydrocarbon chains and by *sn*-1 linkage. Moreover, a comparison based on headgroup (Fig. 7) indicates that at the physiologically relevant π of 35 mN/m, these structural features also regulate C_s^{-1} of otherwise identical molecules. Examination of Fig. 7 shows that as the modulus value decreases, the difference between experimental values and the theoretical line of identity decreases; and the point of coincidence can be calculated to occur at C_{s35}^{-1} of 110 mN/m. For a similar plot, obtained when C_{s35}^{-1} values of esters and vinyl ethers were compared (not shown), coincidence occurs at 84 mN/m. Inspection of the data (Tables 3 and 4) on which the plots are based reveals that lower values of the modulus are associated with increasing chain unsaturation and, hence, larger A_{35}. This trend raises the question of whether at $C_{s35}^{-1} < 100$ mN/m, e.g., for molecules with even larger A_{35}, the linkage- and headgroup-based differences might disappear and the chains might dominate C_{s35}^{-1}. Table 2 and Fig. 7 (*solid triangle*) show that the values for DhDhPC (98 mN/m) and DhDhPE (94 mN/m) are similar, consistent with this prediction. Because the highly unsaturated compounds have the highest A_{35} values and lowest C_{s35}^{-1} values of all molecular pairs studied, the independence of C_s^{-1} from differences in linkage and headgroup at $C_s^{-1} < 100$ mN/m cannot be directly tested at 35 mN/m. However, C_s^{-1} also decreases with decreasing π, so it is possible to compare C_s^{-1} at a $\pi < 35$ mN/m, i.e., larger molecular areas. If that data were to shift to the line of identity, it would indicate that linkage and headgroup regulate C_s^{-1} only when the molecules are closely packed. Such plots (not shown) retain the same type of deviation from the line of identity shown in Fig. 7, even when π is chosen such that none of the C_s^{-1} values exceeds 40 mN/m. This suggests that C_s^{-1} is at all areas determined primarily by the behavior of the hydrated part of the surface. Indeed, if one calculates the modulus using the hydrated area, A_{35}-A_∞, in place of A_{35} and compares species that contain PC with species that contain PE as in Fig. 7, the C_{s35}^{-1} values for comparable species give an offset plot in which the C_{s35}^{-1} data are approximately parallel to the line of identity but offset by ~6 mN/m (not shown). This strongly suggests that most of the differences in compressional moduli arise from the larger hydrated areas of PC-containing species relative to those of PE-containing species at any given surface pressure (42). A similar transformation is observed for vinyl ethers versus acyl lipids if these A_∞-corrected moduli are compared on the basis of *sn*-1 linkage. However, the ethers fall on the line of identity (not shown). The ability of these plots to bring the C_{s35}^{-1} data close and parallel to the line of identity indicates that the fitting parameter, A_∞, truly represents the incompressible part of each lipid molecule, consistent with its conceptual meaning in the equation of state from which A_∞ is obtained.

If the hydrated part of the lipid molecule determines C_s^{-1}, then the value of C_s^{-1} or the derivative from which it is calculated, ($d\pi/dA$), should show a dependence to the water activity parameter, f_1. Fig. 9 shows that $d\pi/dA_{35}$ varies linearly ($R = 0.982$) with f_1 for all 28 compounds included in this study (Tables 2–4). This linear relation is not directly predicted by differentiating the equation of state with which f_1 and A_∞ are calculated from each π-A isotherm. So, it must be a consequence of a degeneracy that occurs with the particular values of the parameters for these phosphoglycerides. A linear correlation was also observed when C_{s35}^{-1} rather than $d\pi/dA_{35}$ values were plotted against f_1 (not shown, $R = 0.967$). Moreover, addition to Fig. 9 of the nine phosphoglycerides from our previous study (16) that have not been discussed herein, had little effect on Fig. 8 (not shown, $R = 0.966$). Included in these are diacyl species having *sn*-2-esterified Dh, Ar, and O; and *sn*-3-esterified PS, PI, and phosphate headgroups. Given the range of headgroup and chain structures covered in this and the previous study, the relationship shown in Fig. 9 is likely universal for biologically relevant phosphoglyceride classes exhibiting liquid-expanded (fluid) monolayer states.

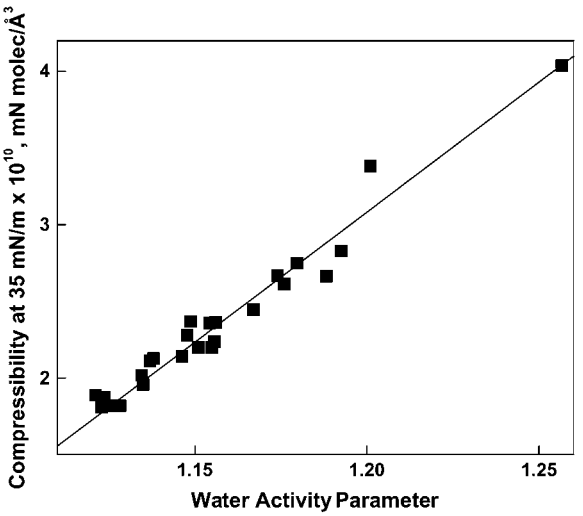

FIGURE 9 Relationship between the water activity parameter of a phosphoglyceride species and its compressibility at 35 mN/m. Values of $d\pi/dA_{35}$, the slope of the π-A isotherm of a phosphoglyceride at 35mN/m, are plotted against the value of f_1 for that species. The line shows a least-squares fit of the data taken from Tables 2–4.

Overall, this and the previous study show that the electrostatic properties of phosphoglyceride molecular species are surprisingly modular in that headgroup, linkage to glycerol, and chain structure make essentially independent contributions to total values of $\mu_\perp$. The modularity of dipole moments supports and extends the partial molecular dipole analysis of Demchak and Fort (43). However, this study improves the earlier analysis by including the correction for ΔV_0 (26). Additionally, it shows that the contributions of functional groups to the mechanical properties of lipid monolayers exhibit modularity. As a consequence, molecular species of phosphoglycerides that differ in one or more structural features can have special physical properties, as we have shown for *sn*-1-Dh-2-Dh molecular species (which have larger molecular areas, are more compressible, and have lower dipole moments than corresponding *sn*-1-S-2-Dh molecular species); PC-containing molecular species (which are generally more compressible than the corresponding PE-containing molecular species); and *sn*-1-Oe-2-acylPE-containing phosphoglycerides (which have lower molecular areas, compressibilities, and dipole moments than the corresponding *sn*-1-S-2-acyl or *sn*-1-Od-2-acyl molecular species). The significance of this complexity for mammalian cell membranes remains to be clarified; but, as a starting point, it might be possible to address this issue by studying the interactions of special proteins and phosphoglycerides that are known to be present in membranes that have special functions.

CONCLUSION

Clearly, physical studies of Dh-containing phosphoglycerides and their interactions with integral and peripheral membrane proteins will continue to advance our understanding of why Dh and related species accumulate in specific tissues and why they are often highly conserved. However, such studies must increasingly recognize, as demonstrated in this work, that seemingly small structural differences between phosphoglyceride species can significantly alter packing and electrostatic properties. This means that we must gain a better understanding of the phosphoglyceride species composition of membranes that contain particular proteins to reveal how the phosphoglyceride species and proteins act together to regulate function.

The authors thank R. E. Brown for helpful comments.

This work was supported by the Howard Hughes Medical Institute (J.A.G.), United States Public Health Service grant No. HL49180 (H.L.B.), and the Hormel Foundation (H.L.B.).

REFERENCES

1. Niu, S.-L., D. C. Mitchell, S.-Y. Lim, Z.-M. Wen, H.-Y. Kim, N. Salem, Jr., and B. J. Litman. 2004. Reduced G protein-coupled signaling efficiency in retinal rod outer segments in response to *n*-3 fatty acid deficiency. *J. Biol. Chem.* 279:31098–31104.
2. Darin-Bennett, A., A. Poulos, and I. G. White. 1976. Fatty acid composition of major phosphoglycerides of ram and human spermatozoa. *Andrologia.* 8:37–45.
3. Lin, D. S., W. E. Connor, D. P. Wolf, M. Neuringer, and D. L. Hachey. 1993. Unique lipids of primate spermatozoa: desmosterol and docosahexaenoic acid. *J. Lipid Res.* 34:491–499.
4. Han, X., D. M. Holtzman, and D. W. McKeel, Jr. 2001. Plasmalogen deficiency in early Alzheimer's disease subjects and in animal models: molecular characterization using electrospray ionization mass spectrometry. *J. Neurochem.* 77:1168–1180.
5. Murthy, M., J. Hamilton, R. S. Greiner, T. Moriguchi, N. Salem, Jr., and H.-Y. Kim. 2002. Differential effects of n-3 fatty acid deficiency on phospholipid molecular species composition in the rat hippocampus. *J. Lipid Res.* 43:611–617.
6. Neuringer, M., W. E. Connor, C. Van Petten, and L. Barstad. 1984. Dietary omega-3 fatty acid deficiency and visual loss in infant Rhesus monkeys. *J. Clin. Invest.* 73:272–276.
7. Connor, W. E., R. G. Weleber, C. DeFrancesco, D. S. Lin, and D. P. Wolf. 1997. Sperm abnormalities in retinitis pigmentosa. *Invest. Ophthalm. Vis. Sci.* 38:2619–2628.
8. Connor, W. E., D. S. Lin, D. P. Wolf, and M. Alexander. 1998. Uneven distribution of desmosterol and docosahexaenoic acid in the heads and tails of monkey sperm. *J. Lipid Res.* 39:1404–1411.
9. McCann, J. C., and B. N. Ames. 2005. Is docosahexaenoic acid, an n-3 long-chain polyunsaturated fatty acid, required for development of normal brain function? An overview of evidence from cognitive and behavioral tests in humans and animals. *Am. J. Clin. Nutr.* 82:281–295.
10. Lauritzen, L., H. S. Hansen, M. H. Jørgensen, and K. F. Michaelsen. 2001. The essentiality of long chain *n*-3 fatty acids in relation to development and function of the brain and retina. *Prog. Lipid Res.* 40:1–94.
11. Alessandri, J.-M., P. Guesnet, S. Vancassel, P. Astorg, I. Denis, B. Langelier, S. Aïd, C. Poumès-Ballihaut, G. Champeil-Potokar, and M. Lavialle. 2004. Polyunsaturated fatty acids in the central nervous system: evolution of concepts and nutritional implications throughout life. *Repro. Nutr. Dev.* 44:509–538.
12. Glomset, J. A. 2006. Role of docosahexaenoic acid in neuronal plasma membranes. *Sci. STKE.* 321:pe6.
13. Gawrisch, K., N. V. Eldho, and L. L. Holte. 2003. The structure of DHA in phospholipid membranes. *Lipids.* 38:445–452.

14. Stillwell, W., and S. R. Wassall. 2003. Docosahexaenoic acid: membrane properties of a unique fatty acid. *Chem. Phys. Lipids*. 126:1–27.

15. Feller, S. E., and K. Gawrisch. 2005. Properties of docosahexaenoic-acid-containing lipids and their influence on the function of rhodopsin. *Curr. Opin. Struct. Biol*. 15:416–422.

16. Brockman, H. L., K. R. Applegate, M. M. Momsen, W. C. King, and J. A. Glomset. 2003. Packing and electrostatic behavior of *sn*-2-docosahexaenoyl and -arachidonoyl phosphoglycerides. *Biophys. J*. 85:2384–2396.

17. Brockman, H. L. 1994. Dipole potential of lipid membranes. *Chem. Phys. Lipids*. 73:57–79.

18. Gross, R. W. 1984. High plasmalogen and arachidonic acid content of canine myocardial sarcolemma: a fast atom bombardment mass spectroscopic and gas chromatography-mass spectroscopic characterization. *Biochemistry*. 23:158–165.

19. Vecchini, A., F. Del Rosso, L. Binaglia, N. S. Dhalla, and V. Panagia. 2000. Molecular defects in sarcolemmal glycerophospholipid subclasses in diabetic cardiomyopathy. *J. Mol. Cell. Cardiol*. 32:1061–1074.

20. Bartlett, G. R. 1959. Phosphorus assay in column chromatography. *J. Biol. Chem*. 234:466–469.

21. Lee, S., D. H. Kim, and D. Needham. 2001. Equilibrium and dynamic interfacial tension measurements at microscopic interfaces using a micropipette technique. 2. Dynamics of phospholipid monolayer formation and equilibrium tensions at the water-air interface. *Langmuir*. 17:5544–5550.

22. Feng, S., H. L. Brockman, and R. C. MacDonald. 1994. On osmotic-type equations of state for liquid-expanded monolayers of lipids at the air-water interface. *Langmuir*. 10:3188–3194.

23. Smaby, J. M., and H. L. Brockman. 1991. An evaluation of models for surface pressure-area behavior of liquid-expanded monolayers. *Langmuir*. 7:1031–1034.

24. MacDonald, R. C. 1996. The relationship and interactions between lipid bilayers vesicles and lipid monolayers at the air/water interface. *In* Vesicles. M. Rosoff, editor. Marcel Dekker, New York.

25. Marsh, D. 1996. Lateral pressure in membranes. *Biochim. Biophys. Acta*. 1286:183–223.

26. Smaby, J. M., and H. L. Brockman. 1990. Surface dipole moments of lipids at the argon-water interface. Similarities among glycerol-ester-based lipids. *Biophys. J*. 58:195–204.

27. Brockman, H. L., M. M. Momsen, R. E. Brown, L. He, J. Chun, H.-S. Byun, and R. Bittman. 2004. The 4,5-double bond of ceramide regulates its dipole potential, elastic properties, and packing behavior. *Biophys. J*. 87:1722–1731.

28. Seelig, J., P. M. Macdonald, and P. G. Scherer. 1987. Phospholipid headgroups as sensors of electric charge in membranes. *Biochemistry*. 26:7535–7541.

29. Han, X., and R. W. Gross. 1990. Plasmenylcholine and phosphatidylcholine membrane bilayers possess distinct conformational motifs. *Biochemistry*. 29:4992–4996.

30. Dyck, M., P. Krüger, and M. Lösche. 2005. Headgroup organization and hydration of methylated phosphatidylethanolamines in Langmuir monolayers. *Phys. Chem. Chem. Phys*. 7:150–156.

31. Phillips, M. C., D. E. Graham, and H. Hauser. 1975. Lateral compressibility and penetration into phospholipid monolayers and bilayer membranes. *Nature*. 254:154–156.

32. McIntosh, T. J., and S. A. Simon. 2006. Roles of bilayer material properties in function and distribution of membrane proteins. *Annu. Rev. Biophys. Biomol. Struct*. 35:177–198.

33. Vogel, V., and D. Möbius. 1988. Local surface potentials and electric dipole moments of lipid monolayers: contributions of the water/lipid and the lipid/air interfaces. *J. Colloid Interface Sci*. 126:408–420.

34. Eldho, N. V., S. E. Feller, S. Tristram-Nagle, I. V. Polozov, and K. Gawrisch. 2003. Polyunsaturated docosahexaenoic vs. docosapentaenoic acid—differences in lipid matrix properties from the loss of one double bond. *J. Am. Chem. Soc*. 125:6409–6421.

35. Disalvo, E. A., F. Lairion, F. Martini, M. A. Frias, S. B. Diaz, and E. E. Tymczyszyn. 2007. Water of hydration and confined water are relevant for the structural and functional properties of biomembranes. *Biophys. J*. 92:1114-Pos.(Abstr.)

36. Berkowitz, M. L., D. L. Bostick, and S. Pandit. 2006. Aqueous solutions next to phospholipid membrane surfaces: insights from simulations. *Chem. Rev*. 106:1527–1539.

37. Paltauf, F. 1994. Ether lipids in biomembranes. *Chem. Phys. Lipids*. 74:101–139.

38. Applegate, K. R., and J. A. Glomset. 1991. Effect of acyl chain unsaturation on the packing of model diacylglycerols in simulated monolayers. *J. Lipid Res*. 32:1645–1655.

39. Clarke, R. J. 2001. The dipole potential of phospholipid membranes and methods for its detection. *Adv. Colloid Interface Sci*. 89:263–281.

40. Smaby, J. M., A. Hermetter, P. C. Schmid, F. Paltauf, and H. L. Brockman. 1983. Packing of ether and ester phospholipids in monolayers. Evidence for hydrogen bonded water at the *sn*-1 acyl group of phosphatidylcholines. *Biochemistry*. 22:5808–5813.

41. Gawrisch, K., D. Ruston, J. Zimmerberg, V. A. Parsegian, R. P. Rand, and N. Fuller. 1992. Membrane dipole potentials, hydration forces, and the ordering of water at membrane surfaces. *Biophys. J*. 61:1213–1223.

42. Pohle, W., D. R. Gauger, M. Bohl, E. Mrazkova, and P. Hobza. 2004. Lipid hydration: headgroup CH moieties are involved in water binding. *Biopolymers*. 74:27–31.

43. Demchak, R. J., and T. Fort, Jr. 1974. Surface dipole moments of close-packed un-ionized monolayers at the air-water interface. *J. Colloid Interface Sci*. 46:191–202.